ISSN 1674-1056
http://cpb.iphy.ac.cn
http://iopscience.iop.org/cpb
中国物理 B
Chinese Physics
中国物理 Chinese Physics B

Observation of hopping transitions for delocalized electrons by temperature-dependent conductance in siliconjunctionless nanowire transistors

Yang-Yan Guo(郭仰岩)[1,2], Wei-Hua Han(韩伟华)[1,2], Xiao-Song Zhao(赵晓松)[1,2], Ya-Mei Dou(窦亚梅)[1,2], Xiao-Di Zhang(张晓迪)[1,2], Xin-Yu Wu(吴歆宇)[1,2], Fu-Hua Yang(杨富华)[1,2,3]

Citation: Chin. Phys. B . 2019, 28(10): 107303 . **doi:** 10.1088/1674-1056/ab3e68
Journal homepage: http://cpb.iphy.ac.cn; http://iopscience.iop.org/cpb

What follows is a list of articles you may be interested in

Multi-step shot noise spectrum induced by a local large spin

Niu Peng-Bin, Shi Yun-Long, Sun Zhu, Nie Yi-Hang
Chin. Phys. B . 2015, 24(12): 127309 . **doi:** 10.1088/1674-1056/24/12/127309

Two-electron localization in a quantum dot molecule driven by a cosine squared field

Zhong Guang-Hui, Wang Li-Min
Chin. Phys. B . 2015, 24(4): 047306 . **doi:** 10.1088/1674-1056/24/4/047306

Fano-type resonances induced by a boson mode in Andreev conductance

J. Barański, T. Domański
Chin. Phys. B . 2015, 24(1): 017304 . **doi:** 10.1088/1674-1056/24/1/017304

Temperature-controllable spin-polarized current and spin polarization in a Rashba three-terminal double-quantum-dot device

Hong Xue-Kun, Yang Xi-Feng, Feng Jin-Fu, Liu Yu-Shen
Chin. Phys. B . 2013, 22(5): 057306 . **doi:** 10.1088/1674-1056/22/5/057306

Transport through artificial single-molecule magnets: Spin-pair state sequential tunneling and Kondo effects

Niu Peng-Bin, Wang Qiang, Nie Yi-Hang
Chin. Phys. B . 2013, 22(2): 027307 . **doi:** 10.1088/1674-1056/22/2/027307

Observation of hopping transitions for delocalized electrons by temperature-dependent conductance in silicon junctionless nanowire transistors*

Yang-Yan Guo(郭仰岩)[1,2], Wei-Hua Han(韩伟华)[1,2,†], Xiao-Song Zhao(赵晓松)[1,2], Ya-Mei Dou(窦亚梅)[1,2], Xiao-Di Zhang(张晓迪)[1,2], Xin-Yu Wu(吴歆宇)[1,2], and Fu-Hua Yang(杨富华)[1,2,3]

[1] *Engineering Research Center for Semiconductor Integrated Technology & Beijing Engineering Center of Semiconductor Micro-Nano Integrated Technology, Institute of Semiconductors, Chinese Academy of Sciences, Beijing* 100083, *China*

[2] *Center of Materials Science and Optoelectronics Engineering, University of Chinese Academy of Sciences, Beijing* 100049, *China*

[3] *State Key Laboratory for Superlattices and Microstructures, Institute of Semiconductors, Chinese Academy of Sciences, Beijing* 100083, *China*

(Received 12 June 2019; revised manuscript received 14 August 2019; published online 17 September 2019)

We demonstrate transitions of hopping behaviors for delocalized electrons through the discrete dopant-induced quantum dots in n-doped silicon junctionless nanowire transistors by the temperature-dependent conductance characteristics. There are two obvious transition platforms within the critical temperature regimes for the experimental conductance data, which are extracted from the unified transfer characteristics for different temperatures at the gate voltage positions of the initial transconductance g_m peak in V_{g1} and valley in V_{g2}. The crossover temperatures of the electron hopping behaviors are analytically determined by the temperature-dependent conductance at the gate voltages V_{g1} and V_{g2}. This finding provides essential evidence for the hopping electron behaviors under the influence of thermal activation and long-range Coulomb interaction.

Keywords: junctionless nanowire transistors, temperature-dependent conductance, variable range hopping, localization length

PACS: 73.63.Kv, 72.20.Ee, 71.23.An, 85.30.Tv **DOI:** 10.1088/1674-1056/ab3e68

1. Introduction

The prospect of atom-scale transistor has been initially indicated by single atom transistor, in which a single phosphorus atom as a quantum dot is high-precisely positioned between source and drain leads by the probe lithography.[1–5] Many notable approaches toward atomic electronic devices have also been explored.[6–9] As the channel width of the silicon transistor is scaled down to several nanometers, few ionized dopant atoms randomly distributed in the channel can work as quantum dots (QDs) and play a significant role in the electron transport behaviors.[10–14] In recent years, single-electron tunneling through the dopant-induced QD array has attracted much attention in the study of the silicon junctionless nanowire transistors (JNTs), which may provide a one-dimensional bulk channel with an adjustable width by the gate electric field.[7,15,16] The conducting path in the center of the silicon nanowire, which is effectively confined by the surface depletion potentials, can be gradually broadened to the whole conduction channel region with the increase of the gate voltage.[17] Few dopant atoms would be discrete in the extremely narrow channel at the initial gate voltages. Therefore, it is very necessary to further understand the thermally activated electron hopping through discrete dopant-induced QDs in the extremely narrow channel. At low temperatures, the silicon JNTs show that the conductance features evolve from clear oscillatory peaks to several steps with the channel broadening, which reflect the electrons successively passing through the impurity levels of the dopant-induced QDs and the conduction subbands of the quantum wire.[18,19] With temperature increasing, the conductance features can be smeared due to thermal broadening by the scattering of thermally activated electrons, which are delocalized from the ionized dopant atoms.[20] In this paper, we demonstrate transitions of hopping behaviors for delocalized electrons through the discrete dopant-induced quantum dots in n-doped silicon junctionless nanowire transistors by the temperature-dependent conductance characteristics. We find two obvious transition platforms within the critical temperature regimes for the experimental conductance data, which are extracted from the unified transfer characteristics for different temperatures at the gate voltage positions of the initial transconductance g_m peak in V_{g1} and valley in V_{g2}. The crossover temperatures of electron hopping behaviors are analytically determined by the temperature-dependent conductance at the gate voltages V_{g1} and V_{g2}.

2. Device fabrication and characterization

The schematic structure of the silicon JNT device for investigation is provided in Fig. 1(a). The fabrication of the

*Project supported by the National Key R&D Program of China (Grant No. 2016YFA0200503) and the National Natural Science Foundation of China (Grant No. 61327813).

†Corresponding author. E-mail: weihua@semi.ac.cn

© 2019 Chinese Physical Society and IOP Publishing Ltd

silicon JNT device started from a boron-doped (10^{15} cm^{-3}) (100)-oriented silicon-on-insulator (SOI) wafer with 55-nm-thick top silicon layer and 145-nm-thick buried oxide layer. After growing a 18-nm-thick thermal oxidation layer, the top silicon layer was uniformly doped by phosphorus ion implantation with a dose of 2 $\times 10^{12}$ cm^{-2} at an energy of 33 keV. A silicon nanowire was defined along ⟨110⟩ direction by electron beam lithography (EBL) and inductively coupled plasma (ICP) etching, followed by a sacrificial oxidation to eliminate the etching-induced damages. Then 22-nm-thick gate oxide layer was grown by thermal oxidation at the temperature of 900 ℃ in dry oxygen. The 200-nm-thick polysilicon layer was deposited by low-pressure chemical vapor deposition (LPCVD). After heavily doped by boron ion implantation, the sample was rapidly annealed in nitrogen ambient at 1000 ℃ for 10 s. The polysilicon gate with the length of 280 nm was then defined by electron beam overlay exposure and dry etching, conformally wrapping the Si/SiO_2 core–shell nanowire. Finally, it was followed by the deposition of 200 nm-thick SiO_2 passivation layer, standard metal contact formation, and sintering. The SEM image of the single-channel JNT in Fig. 1(b) shows the width of 58 nm for the Si/SiO_2 core–shell nanowire. As a result, we may estimate that the silicon core has the physical width of about 14 nm and the height of about 26 nm. The dopant concentration in the silicon channel after several times annealing is estimated to be 4.16×10^{17} cm^{-3} according to the implantation dose of phosphorus ions. The fabricated device was measured in a vacuum chamber which can be cooled down to the low temperature of 6 K with the help of Lakershore-340 temperature controller.

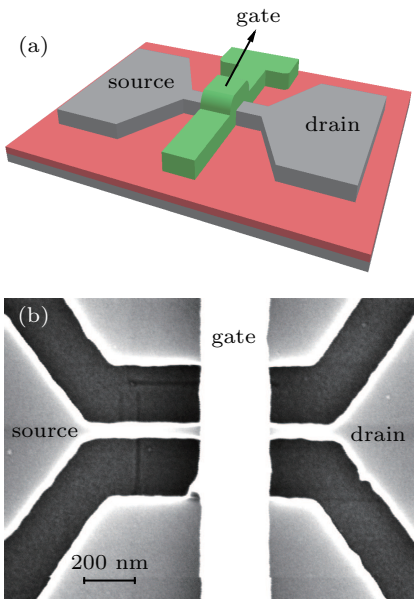


Fig. 1. (a) The schematic structure of silicon JNT. (b) The top-view SEM image of silicon JNT after gate formation.

3. Results and discussion

We study the thermally activated electrons transport behaviors through the discrete dopant-induced QDs in the impurity band of the silicon JNT within the temperature range from 6 K to 250 K by the temperature-dependent conductance characteristics of the silicon JNT. The thermally activated electron transport is dominated by phonon-assisted hopping through several dopant-induced QDs.[21] Mott believed that a hopping electron with activation energy E_a would always try to find a lower energy state around the Fermi level by the variable range hopping (VRH) in the absence of long-range Coulomb interaction.[22] At high temperatures, the temperature dependence of conductance G for the nearest neighbor hopping (NNH) exhibits as $G \propto \exp(-E_a/k_B T)$, where k_B is the Boltzmann constant.[23] If the activation energy at low temperatures is reduced as large as the Coulomb interaction energy, the VRH conductance which has been predicted by Efros and Shklovskii (ES) should obey the 1/2 exponent law given by $G \propto \exp[-(T_{ES}/T)^{1/2}]$, where T_{ES} is the temperature-independent ES coefficient.[24] Therefore, with temperature increasing, three kinds of electron hopping transports would be observed in the following consequence: ES-type VRH, Mott-type VRH, and NNH.[21] In our experiment, we find two obvious transition platforms within the critical temperature regimes of A and B for the experimental conductance data, which are extracted from the unified transfer characteristics at the gate voltage positions of the initial transconductance g_m peak in V_{g1} and valley in V_{g2}. One crossover temperature T_A in the higher temperature regime A corresponds to the transition of thermally-activated-electron transport behaviors from NNH to Mott-type VRH.[25] The other crossover temperature T_C in the lower temperature regime B corresponds to the VRH transition for the delocalized electrons from Mott law to the ES law under the influence of Coulomb interaction.[26] The quantitative analysis on the experimental temperature-dependent conductance data has been taken by linear fitting of $\ln G \propto -E_a/k_B T$ for NNH, $\ln G \propto -(T_M/T)^{1/4}$ for Mott-type VRH, and $\ln G \propto -(T_{ES}/T)^{1/2}$ for ES-type VRH.

Figure 2(a) presents the temperature-dependent conductance G (i.e., $G = I_{DS}/V_{DS}$) curves obtained from the transfer characteristics at low source–drain bias $V_{DS} = 1$ mV. The clear quantized current steps below the temperature of 75 K indicate the population of the individual sub-bands caused by the quantum confinement effect.[27] Above the temperature of 75 K, the thermal energy is greater than the subbands spacing, resulting in the smearing of the current steps. Figure 2(b) illustrates the corresponding transconductance g_m–V_G characteristics at different temperatures. We define the onset gate voltage V_{gt} as the initial point of the first g_m peak, where the

drain current in the conduction channel is at the onset state. The onset gate voltage V_{gt} increases from 6 K to 20 K and decreases from 100 K to 250 K, resulting from the interaction of the induced image charges in the dielectric interface with the impurity and the subband states in the channel.[13] To explore the conductance characteristics under the same filled energy level, we take the onset gate voltage V_{gt} to unify the transfer characteristics in Fig. 2(a) for the alignment of energy levels at different temperatures. In order to clarify the electron hopping transport in the impurity band, figure 2(c) shows the I_{DS}–V_g curves (upper part) and the corresponding transconductance g_m–V_g curves (lower part) at the temperature of 6 K under the bias V_{DS} varying from 1 mV to 10 mV. The clear oscillatory current with several splitting peaks (upper part) identifies the coupling of dopant-induced QDs in the impurity band. With the gate voltage increasing, the Fermi energy level of electrons in the quantum confined channel is allowed to enter the conduction subbands, resulting in the current steps.[28,29]

In order to study the temperature-dependent conductance G characteristics in Fig. 2(a), we firstly extract the experimental conductance data for different temperatures according to the initial g_m peak at the gate voltage V_{g1}, in which the effective mobility of hopping electrons is the highest in the impurity band. For comparison, we also provide the temperature-dependent conductance data according to the initial g_m valley at the gate voltage V_{g2}, in which the electron hopping behavior is suppressed by the Coulomb interaction. Figure 2(d) provides the Arrhenius conductance plots (G vs. $1/T$) at the gate voltages of V_{g1} and V_{g2} within the temperature range from 6 K to 250 K. Interestingly, it is found that the conductance at the temperature of 6 K is much larger than that of 10 K, which may be related with the Coulomb interaction. As the temperature increases, the incomplete ionized donors in the channel are gradually transformed into ionized donors, which result in stronger impurity scattering to reduced the electron mobility.[30] The inset G–T diagrams in Fig. 2(d) show two apparent platforms of the conductance for the gate voltages V_{g1} and V_{g2} within the temperature regions of around 200 K and around 100 K, as the color marked A and B. The platform of the temperature-dependent conductance for the gate voltage V_{g1} within the temperature range from 50 K to 100 K is more evident than that of the gate voltage V_{g2} within the temperature range from 75 K to 125 K, resulting from the stronger quantum confinement at the initial stage of the conduction channel in the silicon JNT.

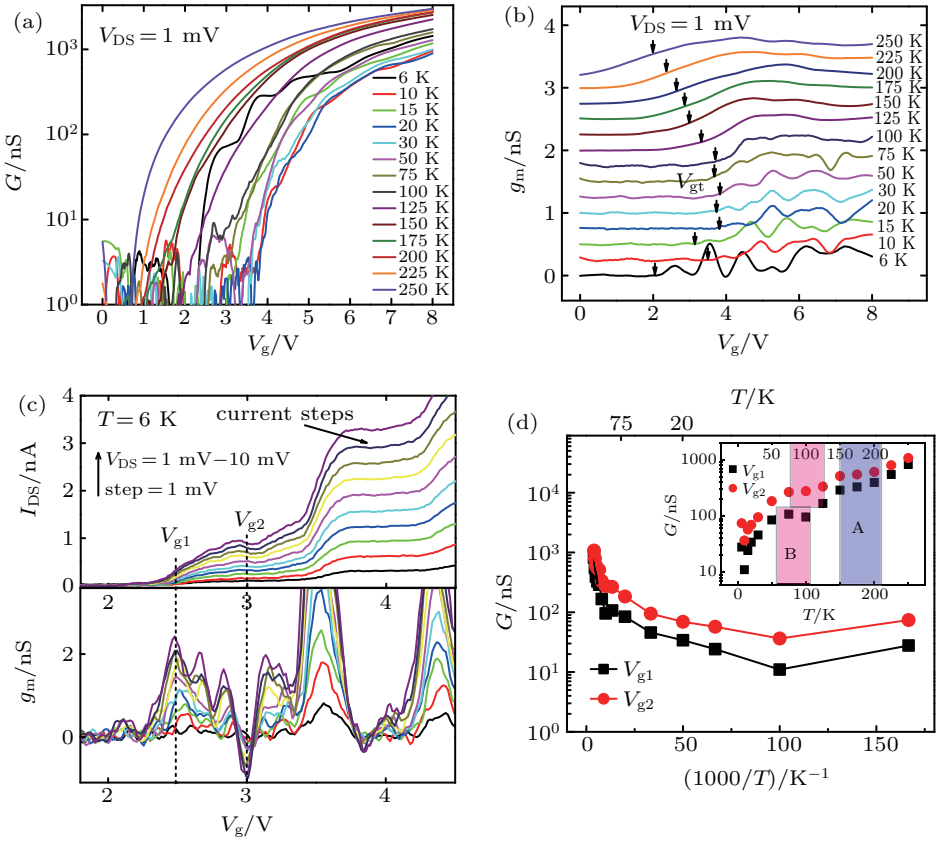


Fig. 2. (a) The temperature-dependent conductance G (i.e., $G = I_{DS}/V_{DS}$) curves of the device at $V_{DS} = 1$ mV within the temperature range from 6 K to 250 K. (b) The temperature-dependent transconductance g_m–V_G characteristics at $V_{DS} = 1$ mV, where the transconductance is given by $g_m = dI_{DS}/dV_G$. (c) I_{DS}–V_g curves (upper part) and the corresponding transconductance g_m–V_g curves (lower part) at the temperature of 6 K under the bias V_{DS} varying from 1 mV to 10 mV. (d) The Arrhenius conductance plots (G vs. $1/T$) on logarithmic scale at the gate voltages of V_{g1} and V_{g2} within the temperature range from 6 K to 250 K, The inset shows the corresponding temperature-dependent conductance data (G vs. T), which are extracted from panel (a) after unified by the onset gate voltage V_{gt} at different temperatures.

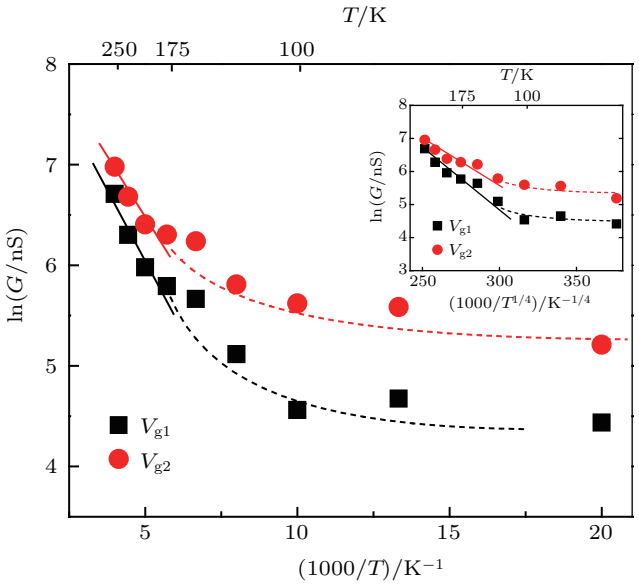


Fig. 3. Arrhenius plot of conductance in $\ln G$ vs. $1/T$ scales for NNH within the temperature range from 175 K to 250 K. The inset shows Mott-type VRH temperature dependence of the conductance in $\ln G$ vs. $(1/T)^{1/4}$ scales.

In order to precisely determine the transition temperatures T_A in temperature region A, we replot the Arrhenius curves of temperature-dependent conductance at high temperature regime as the curves of $\ln G$ vs. $1/T$ in Fig. 3 for the gate voltages V_{g1} and V_{g2} respectively. The inset shows the Mott-type VRH temperature dependence of the conductance in $\ln G$ vs. $(1/T)^{1/4}$ scales. Here, we are interested in the hopping behaviors of the thermally activated electrons from the ionized dopant atoms. The linearly fitting by $\ln G \propto -E_a/k_B T$ is shown in Fig. 3 for the thermally activated electrons by NNH above the crossover temperature T_A, in which the electrons have enough thermal activation energy E_a to overcome the potential barriers between the nearest neighbor states. The hopping distance r in NNH is supposed to be equivalent to the mean distance d between neighbored dopant atoms, which can be determined by the doping concentration N_d as

$$d = (N_d)^{-1/3}. \tag{1}$$

According to the doping concentration $N_d = 4.16 \times 10^{17}$ cm^{-3}, the hopping distance between the nearest neighbored dopant atoms is estimated to be 13.4 nm. According to the linearly fitting of the experimental conductance data in Fig. 3 within the temperature range from 175 K to 250 K, the activation energies E_a for the hopping electrons are extracted to be 45.2 meV and 33.7 meV respectively for the curves at the gate voltages V_{g1} and V_{g2}.[31] According to Mott's theory, the activation energy E_a for electron hopping is related to the constant density of states (DOS) g_0 at the Fermi level and the hopping distance r as[32]

$$E_a = 3/(4\pi g_0 r^3). \tag{2}$$

The probability P for hopping is proportional to the conductance G of the device, which depends on the overlap integral of the wavefunctions within the localization radius a and the activation energy E_a,[26] i.e.,

$$P \propto G \propto \exp(-2r/a - E_a/k_B T). \tag{3}$$

Taking the expression of E_a (Eq. (2)) into Eq. (3), one may get the relation between the probability and the hopping distance, $P \propto G \propto \exp(-2r/a - 3/(4\pi g_0 r^3 k_B T))$. After taking the derivative of the hopping probability $dP/dr = 0$, the optimal electron hopping distance $\bar{r}_M$ is obtained to be[33]

$$\bar{r}_M = (9a_M/8\pi g_0 k_B T)^{1/4}, \tag{4}$$

where a_M is the localization length in the Mott hopping regime. At the crossover temperature T_A, the electron hopping distance of VRH is assumed to be equal to that of NNH,

$$\bar{r}_M|_{T_A} = d. \tag{5}$$

By taking the expression of $\bar{r}_M$ (Eq. (4)) into Eq. (5), we deduce the expression

$$T_A = 9a_M/8\pi g_0 k_B d^4, \tag{6}$$

which is determined by the localization length a_M and the density of states g_0. In order to determine the localization length a_M, we may use the Mott-type VRH conductance expression by substituting Eqs. (2) and (4) into Eq. (3), i.e., $G \propto P \propto \exp(-(T_M/T)^{1/4})$. The temperature factor T_M is related to the localization length a_M by $T_M = 18/g_0 a_M^3 k_B$. According to the fitting results from 175 K to 250 K of $\ln G$ vs. $T^{-1/4}$ scales in the inset of Fig. 3, the temperature factor T_M extracted from the slopes is 38.78^4 K for the gate voltage V_{g1} and 28.9^4 K and for the gate voltage V_{g2}. Therefore, the localization length a_M can be obtained from the expression of T_M be about 3.47 nm and 4.66 nm respectively for the gate voltages V_{g1} and V_{g2}. The density of states g_0 at the Fermi energy can be estimated to be 2.2×10^{18} eV^{-1}·cm^{-3} and 2.96×10^{18} eV^{-1}·cm^{-3} from Eqs. (2) and (5) by taking the activation energies of 45.2 meV and 33.7 meV respectively for the gate voltages V_{g1} and V_{g2}, both of which have the same magnitude as reported in silicon nanowires.[19] As expected from Eq. (6), we obtain the crossover temperatures of $T_{A1} = 203$ K and $T_{A2} = 202$ K respectively for the gate voltages V_{g1} and V_{g2}, which are consistent with the experimental observation in the conductance platform A of Fig. 2(d). The result shows that the crossover temperature T_A from NNH to VRH is independent of the gate electric field, which may result from the stronger interactions of the thermally activated electrons.

In order to understand the transition of the conductance at temperature T_C, we provide the Arrhenius plot of conductance in $\ln G$ vs. $(1/T)^{1/2}$ scales by linear fitting in Fig. 4. With the

temperature decreasing below 150 K, the activation energy extracted from Fig. 2(d) is further reduced to be about 0.84 meV and 0.68 meV respectively for the gate voltages V_{g1} and V_{g2}, by which the VRH at the vicinity of Fermi level E_F is associated with the long-range Coulomb interaction of the dopant-induced QD array. If the energy of each dopant site depends on distribution of other charged dopants, the electrons localized on the states near the Fermi level will be redistributed. The long-range Coulomb interaction energy $\Delta = e^2/4\pi\varepsilon_0\varepsilon_r r$ could reduce the DOS for the electrons localized on the states of QDs around the Fermi level, in which the number of states is given by $N \approx \left(4\pi r^3/3\right)^{-1}$. In order to estimate the DOS near the Fermi level, ES-type VRH model considers that the Coulomb interaction energy Δ is comparable to the activation energy $E_a = E - E_F$. Then, the DOS near the Fermi level is given by[21]

$$g(E) = \frac{dN}{dE} \approx 0.72\left(4\pi\varepsilon_0\varepsilon_r/e^2\right)^3 (E - E_F)^2, \tag{7}$$

whose curve is shown in the inset of Fig. 4. At the crossover temperature T_C for the VRH transition from Mott-type law to ES-type law, the activation energy E_a should be equivalent to the Coulomb interaction energy Δ, i.e.,

$$E_a = \Delta = e^2/4\pi\varepsilon_0\varepsilon_r r. \tag{8}$$

The DOS at the condition of $E_a = \Delta$ would remain constant as g_0 in Mott VRH, which is given by

$$g(E_a) = g(\Delta) = g_0. \tag{9}$$

Then, the hopping distance $\bar{r}_{ES}$ of ES-type VRH can be estimated by the maximum hopping probability[33] of Eq. (3) as

$$\bar{r}_{ES} = \left[e^2 a_{ES}/2(4\pi\varepsilon_0\varepsilon_r) k_B T\right]^{1/2}, \tag{10}$$

in which the localized length a_{ES} in ES hopping regime indicates the average modulation length of long-range Coulomb interaction between the dopant-induced QDs in the conduction channel. In order to determine the localization length a_{ES}, we substitute Eqs. (8) and (10) into Eq. (3) to get the ES-type VRH conductance expression

$$G \propto P \propto \exp(-(T_{ES}/T)^{1/2}). \tag{11}$$

The temperature factor T_{ES} is related to the localization length a_{ES} by

$$T_{ES} = (8e^2/4\pi\varepsilon_0\varepsilon_r a_{ES} k_B). \tag{12}$$

The temperature factor T_{ES} extracted from the slopes is 34.8 K for the gate voltage V_{g1} and 31.4 K for the gate voltage V_{g2}. Therefore, the localization length a_{ES} for ES-type VRH can be obtained from Eq. (12) to be about 323 nm and 358 nm respectively for the gate voltages V_{g1} and V_{g2}. The result indicates that the localization length a_{ES} is enhanced with the increase of the gate voltage due to screening of the trapping potentials of the dopant atoms. Considering the expressions from Eq. (7) to Eq. (10), we finally obtain the expression of T_C,

$$T_C = 0.7e^4 a_{ES} g_0/(4\pi\varepsilon_0\varepsilon_r)^2 k_B, \tag{13}$$

which is determined by the constant DOS g_0 and the localized length a_{ES}. As a result, the crossover temperature of the VRH conductance transition from Mott-type law to ES-type law can be estimated to be $T_{C1} = 85$ K at the gate voltage V_{g1} and $T_{C2} = 126$ K at the gate voltage V_{g2}. Both the two crossover temperatures T_{C1} and T_{C2} are consistent with the experimental observation of conductance platform B of Fig. 2(d). The crossover temperature T_{C2} of 126 K is much higher than T_{C1} of 85 K, which may result from the stronger Coulomb interaction at the gate voltage V_{g2} of the g_m valley.

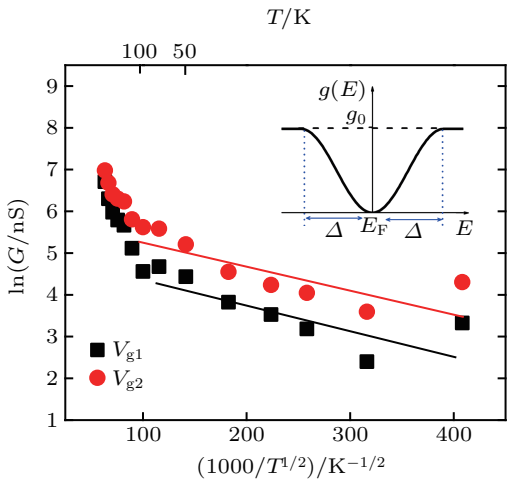


Fig. 4. Arrhenius plot of conductance in $\ln G$ vs. $(1/T)^{1/2}$ scales for ES-type VRH, with the inset for the density of states near the Fermi energy level.

4. Conclusion

We present an experimental evidence of hopping transition for the delocalized electrons in silicon JNT by the temperature-dependent conductance characteristics. The theoretical models of Mott-type VRH and ES-type VRH agree well with the experimental data of temperature-dependent conductance, which are extracted from transfer characteristics for different temperatures at the gate voltage positions of the initial transconductance g_m peak in V_{g1} and the valley in V_{g2}. The crossover temperature T_A from NNH to Mott VRH is analytically determined to be 203 K and 202 K constantly for the gate voltages V_{g1} and V_{g2} by the conductance transition of the thermally activated electrons. Another crossover temperature T_C of VRH behavior from Mott-type law to ES-type law is theoretically determined to be 85 K and 126 K respectively for the

gate voltages V_{g1} and V_{g2} by considering the Coulomb interactions. As expected, stronger Coulomb interaction at the gate voltage V_{g2} of the g_m valley leads to the obvious increase of the crossover temperature T_C for the VRH transition behavior. Our finding provides essential evidence for the hopping electron behaviors under the influence of thermal activation and long-range Coulomb interaction.

Acknowledgment

The authors acknowledge Dr. Hao Wang, Dr. Liuhong Ma, and Mr. Xiaoming Li for their supports in device fabrication.

References

[1] Samanta A, Muruganathan M, Hori M, Ono Y, Mizuta H, Tabe M and Moraru D 2017 *Appl. Phys. Lett.* **110** 093107
[2] Jehl X, Niquet Y M and Sanquer M 2016 *J. Physics.: Condens. Matter* **28** 103001
[3] Tabe M, Moraru D, Ligowski M, Anwar M, Jablonski R, Ono Y and Mizuno T 2010 *Phys. Rev. Lett.* **105** 016803
[4] Pierre M, Wacquez R, Jehl X, Sanquer M, Vinet M and Cueto O 2010 *Nat. Nanotechnol.* **5** 133
[5] Moraru D, Udhiarto A, Anwar M, Nowak R, Jablonski R, Hamid E, Tarido J C, Mizuno T and Tabe M 2011 *Nanoscale Research Letters* **6** 479
[6] Dagesyan S A, Shorokhov V V, Presnov D E, Soldatov E S, Trifonov A S and Krupenin V A 2017 *Nanotechnol.* **28** 225304
[7] Uddin W, Georgiev Y M, Maity S and Das S 2017 *J. Phys. D: Appl. Phys.* **50** 365104
[8] Enrico Prati M H, Filippo Guagliardo, Giorgio Ferrari and Takahiro Shinada 2012 *Nat. Nanotechnol.* **7** 443
[9] Hamid E, Moraru D, Tarido J C, Miki S, Mizuno T and Tabe M 2010 *Appl. Phys. Lett.* **97** 262101
[10] Hori M, Shinada T, Ono Y, Komatsubara A, Kumagai K, Tanii T, Endoh T and Ohdomari I 2011 *Appl. Phys. Lett.* **99** 062103
[11] Sellier H, Lansbergen G P, Caro J, Rogge S, Collaert N, Ferain I, Jurczak M and Biesemans S 2006 *Phys. Rev. Lett.* **97** 206805
[12] Tabe M, Moraru D, Ligowski M, Anwar M, Yokoi K, Jablonski R and Mizuno T 2010 *Thin Solid Films* **518** S38
[13] Wang H, Han W, Ma L, Li X, Hong W and Yang F 2014 *Appl. Phys. Lett.* **104** 133509
[14] Su L N , Lv L, Li X X , Qin H and Gu X F 2015 *Chin. Phys. Lett.* **32** 047301
[15] Rueß F J, Micolich A P, Pok W, Goh K E J, Hamilton A R and Simmons M Y 2008 *Appl. Phys. Lett.* **92** 052101
[16] Pichon L, Jacques E, Rogel R, Salaun A C and Demami F 2013 *Semicond. Sci. Technol.* **28** 025002
[17] Colinge J P, Lee C W, Afzalian A, Akhavan N D, Yan R, Ferain I, Razavi P, O'Neill B, Blake A, White M, Kelleher A M, McCarthy B and Murphy R 2010 *Nat. Nanotechnol.* **5** 225
[18] Ma L, Han W, Wang H, Hong W, Lyu Q, Yang X and Yang F 2015 *J. Appl. Phys.* **117** 034505
[19] Wang H, Han W, Li X, Zhang Y and Yang F 2014 *J. Appl. Phys.* **116** 124505
[20] Barrett C, Lederer D, Redmond G, Xiong W, Colinge J P and Quinn A J 2010 *Solid-State Electron.* **54** 1273
[21] Shlimak I 2015 *Is Hopping A Science* (Singapore: World Scientific) p. 25
[22] M F Kaveh N F M 1983 *Philos. Mag. B* **47** 577
[23] Boris I and Shklovskii A L E 1984 *Electronic Properties of Doped Semiconductors* (Berlin: Springer-Verlag) p. 191
[24] Efros A L and Shklovskii B I 1975 *Journal of Physics C: Solid State Physics* **8** L49
[25] Qiu H, Xu T, Wang Z, Ren W, Nan H, Ni Z, Chen Q, Yuan S, Miao F, Song F, Long G, Shi Y, Sun L, Wang J and Wang X 2013 *Nat. Commun.* **4** 2642
[26] Yu D, Wang C, Wehrenberg B L and Guyot-Sionnest P 2004 *Phys. Rev. Lett.* **92** 216802
[27] Ma L H, Han W H, Wang H, Yang X and Yang A F 2015 *IEEE Trans. Elec. Dev* **36** 941
[28] Je M, Han S, Kim I and Shin H 2000 *Solid-State Electron.* **40** 2207
[29] Zhao X H, Guo Y Y, Dou Y M and Yang F H 2018 *Chin. Phys. B* **27** 097310
[30] Li X, Han W, Wang H, Ma L, Zhang Y, Du Y and Yang F 2013 *Appl. Phys. Lett.* **102** 223507
[31] Wang W, Xu G, Chowdhury M D H, Wang H, Um J K, Ji Z, Gao N, Zong Z, Bi C, Lu C, Lu N, Banerjee W, Feng J, Li L, Kadashchuk A, Jang J and Liu M 2018 *Phys. Rev. B* **98** 245308
[32] Mott N F 1969 *Philos. Mag.* **19** 835
[33] Zhang Y, Dai O, Levy M and Sarachik M P 1990 *Phys. Rev. Lett.* **64** 2687